Sustainable Energy & Fuels

A Hybrid Pathway to Biojet Fuel via 2,3-Butanediol

Journal:	*Sustainable Energy & Fuels*
Manuscript ID	SE-ART-03-2020-000480.R1
Article Type:	Paper
Date Submitted by the Author:	21-Apr-2020
Complete List of Authors:	Adhikari, Shiba; Oak Ridge National Laboratory, MSTD Zhang, Junyan; University of Maryland at College Park, Chemical and biomolecular engineering Guo, Qianying; Oak Ridge National Laboratory, Materials Science and Technology Division Unocic, Kinga; Oak Ridge National Laboratory, Materials Science and Technology Division Tao, Ling; National Renewable Energy Laboratory Li, Zhenglong; Oak Ridge National Laboratory, Energy and Transportation Sciences Division

A Hybrid Pathway to Biojet Fuel via 2,3-Butanediol

Shiba P. Adhikari[a], Junyan Zhang[b, c], Qianying Guo[d], Kinga A. Unocic[d], Ling Tao[e], Zhenglong Li[b]*

[a] Material Science and Technology Division, Oak Ridge National Laboratory, 1 Bethel Valley Road, Oak Ridge, TN 37830, USA.

[b] Energy and Transportation Sciences Division, Oak Ridge National Laboratory, 1 Bethel Valley Road, Oak Ridge, TN 37830, USA.

[c] Department of Chemical and Biomolecular Engineering, University of Maryland, 4418 Stadium Dr, College Park, MD 20742, USA.

[d] Center for Nanophase Materials Sciences, Oak Ridge National Laboratory, 1 Bethel Valley Road, Oak Ridge, TN 37830, USA.

[e] National Bioenergy Center, National Renewable Energy Laboratory, 15013 Denver W Pkwy Golden, CO, 80401, USA

Footnotes

*Corresponding author, E-mail: lizhenglong1982@gmail.com; Phone: +1-517-290-9941

†**Electronic Supporting Information (ESI)** available: Supporting information includes scheme, XRD, BET, STEM, TGA, and different reaction results. See DOI: 10.1039/x0xx00000x

Abstract:

Production of biomass-derived sustainable alternative jet fuels (SAJF) has been considered as an important approach to decarbonize the aviation industry but still possesses various challenges in technology advancement, particularly in achieving high carbon efficiency. Here we report a hybrid pathway to SAJF from 2,3-butanediol (2,3-BDO), integrating biologically converting biomass to 2,3-BDO with catalytically upgrading of 2,3-BDO to jet-range hydrocarbons. This pathway is demonstrated to have a high carbon recovery to liquid hydrocarbons from corn stover (25-28%) (74-82% of the theoretical maximum efficiency). The catalytic conversion steps involve 2,3-BDO to C_{3+} olefins, oligomerization, and hydrogenation where the first two steps are the focus of this study. Under optimum reaction conditions (523 K, 115 kPa, 1.0 h^{-1} weight hourly space velocity), 2,3-BDO conversion and C_{3+} olefin selectivity are >97% and 94-98% during 40 h time on stream, respectively. To demonstrate the adaptability of this technology with bio-derived 2,3-BDO, we also investigated the impact of water and other organic coproducts (acetoin and acetic acid) inherited from the fermentation broth on the catalyst performance and product selectivities. We have shown that the catalyst can handle a significant amount of water in the liquid feed (40 wt.% water/60 wt.% 2,3-BDO) and maintain catalyst stability for ~40 h. Acetoin can be converted to similar C_{3+} olefins as 2,3-BDO with complete conversion of acetoin. Co-feeding 10 wt.% acetoin with 2,3-BDO is found to have no impact on 2,3-BDO conversion, C_{3+} olefin selectivity, and catalyst stability. The utilization of organic coproduct like acetoin can help to improve overall carbon conversion efficiency when using real biomass-derived 2,3-BDO. On the other hand, the presence of 10 wt.% acetic acid is shown to drastically inhibit MEK hydrogenation and butene oligomerization as revealed by the increased MEK and butene selectivities, implying the importance of separating organic acids when feeding bio-derived 2,3-BDO. The formed C_3-C_6

olefins from 2,3-BDO are further oligomerized over Amberlyst-36 catalyst to longer-chain hydrocarbons with >70 wt.% jet-range hydrocarbons including predominantly iso-olefins/iso-paraffins. The overall carbon efficiency for the jet-range hydrocarbons is 19-22%, exceeding most of the reported biojet pathways, which makes it a promising approach for SAJF production.

Keywords: Biomass to jet fuel, Hybrid pathway, 2,3-Butanediol, Methyl ethyl ketone

Introduction

The growing awareness in protecting the earth's environment by decreasing CO_2 concentration in the atmosphere has attracted many researchers moving towards renewable energy sources to replace petroleum-based fuels. There is a great thrust for sustainable alternative jet fuels (SAJF) to decarbonize the aviation industry which consumes approximately 1.5-1.7 billion barrels of jet fuel every year.[1] Among various approaches, biomass conversion to jet fuels (also referred as biojet fuels) offers a promising future because it has the potential to reduce greenhouse gas emissions by up to 85% compared to petroleum-based aviation fuels.[2]

Several conversion technologies for biomass to jet fuels have been reported with each of them targeting different types of feedstocks.[3] So far, biomass-derived sugars, alcohols, syngas, and oils have been investigated to upgrade to biojet fuels via a variety of catalytic processes.[1,4,5] Aqueous-phase routes have been investigated by converting biomass-derived sugars to jet-range hydrocarbons via either gamma-valerolactone (GVL)[6–8] or hydroxymethylfurfural (HMF)[9–11] platform using heterogeneous catalysis. Thermochemical routes involve conversion of biomass to intermediates, such as bio-oil or syngas, and followed by catalytic hydrodeoxygenation[12,13] or syngas to jet via alcohol intermediates.[14] The major barriers for economical commercialization of biojet fuels from various pathways still suffer from low carbon yield and high production cost which is a combination of feedstock cost and conversion efficiency, *etc.*[5,15]

Hybrid pathway integrating biochemical and thermal catalytic steps offers the potential to address some of these challenges.[3,16] This route can usually selectively produce the target intermediates (e.g., alcohols, organic acids) from biomass via biological approaches by utilizing the high selectivity nature of biochemical methods.[5,17] These intermediates can be further

converted to jet-range hydrocarbons via thermal catalytic means at fast kinetics. Meanwhile, as the compositions of these intermediates are much less complicated than the original biomass feedstock, the product selectivity and conversion efficiency of the thermal catalytic step can be more readily controlled to the targeted hydrocarbon products, which makes it likely to achieve high carbon efficiency to jet fuel.[18] On the other hand, due to the ability to control the selectivity of target intermediates via biological methods, this type of pathway also has the potential to generate valuable coproducts besides hydrocarbon fuels, which could help to reduce the final fuel selling price due to higher value of these co-products.[16]

Here we report a new hybrid pathway to produce jet-range hydrocarbons via biomass-derived 2,3-butanediol (2,3-BDO), which is usually produced from different biomass feedstocks[19] as well as from syngas and CO_2.[20,21] This platform chemical offers potential to produce cost-competitive high yield of jet fuel because: 1) 2,3-BDO can be produced at high titer (e.g., >100 g/L) due to low toxicity to producing microorganisms,[22,23] which could significantly reduce energy consumption during product separations; 2) comparing with small molecules (e.g., methanol, ethanol), it is easier to produce a high yield of jet-range hydrocarbons (C_8-C_{16}) from 2,3-BDO as it requires fewer steps of C-C bond formation; 3) it offers many opportunities to produce valuable co-products (e.g. methyl ethyl ketone (MEK), butadiene, epoxides)[24–26] which could help to offset the production cost of jet fuel and lower the fuel selling price.[16,27] Despite the varieties of uses in softening agents, plasticizers, polyesters, drugs and cosmetics,[28] the market volume of 2,3-BDO is still very limited.[29] Developing catalytic approaches to produce biojet and coproducts will also help to expand the market of 2,3-BDO as the prospective global market values of key downstream products form 2,3-BDO is reported to be around $43 billion per year.[30]

Our reported pathway involves biomass conversion to 2,3-BDO via pretreatment, hydrolysis, 2,3-BDO fermentation, 2,3-BDO-to-C_{3+} olefins (BTO), oligomerization, hydrogenation and fractionation as shown in Scheme 1. In this study, we focused on the BTO and oligomerization steps to demonstrate the selective production of jet-range hydrocarbons from 2,3-BDO. Copper modified H-ZSM-5 catalyst was investigated for 2,3-BDO conversion to C_{3+} olefins to understand the product distributions under different reaction conditions such as varying reaction temperatures and hydrogen partial pressures. Conversion of 2,3-BDO to olefins (butenes and butadiene) has been investigated before over various catalysts, including aluminosilicates,[31] gamma-Al_2O_3,[26] CsH_2PO_4/SiO_2,[32] ZSM-5 based catalysts,[33,34] however, these studies mainly targeted the production of the single product stream. Here our study focused on maximizing the selectivity of the total C_{3+} olefin mixture by operating at higher hydrogen partial pressure over Cu/ZSM-5, and we further performed the oligomerization of these mixed olefins to demonstrate high yield of jet-range hydrocarbons. More importantly, we extended our study to investigate the impact of water and organic coproducts (acetoin and acetic acid) on the catalytic upgrading of 2,3-BDO, which will help to demonstrate the applicability of this technology to bio-derived 2,3-BDO. The overall carbon efficiency from biomass to liquid hydrocarbon fuels was also analyzed to compare with other biomass to jet processes.

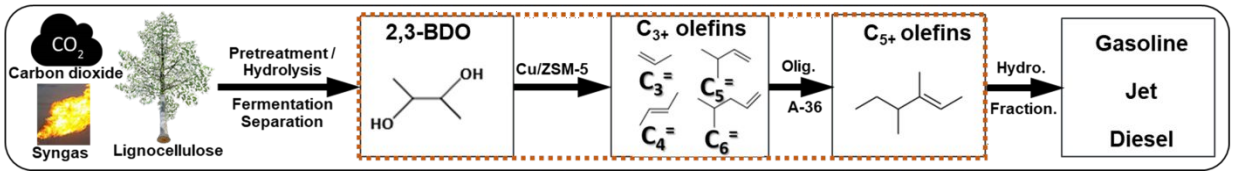

Scheme 1. Hydrocarbon fuel production from bio-derived 2,3-BDO. (A-36 = Amberlyst 36, Olig. = oligomerization, Hydro. = hydrogenation, Fraction. = fractionation). The steps highlighted in the dashed box are the focus of this study.

Experimental section

Materials. The 2,3-butanediol (98%, referred as 'pure 2,3-BDO'), copper nitrate (99%), ammonia solution (28.0-30.0% NH_3 basis), acetic acid (99%), and acetoin (96%) were purchased from Sigma Aldrich. All other chemicals and reagents grade solvents used in this study were obtained from either Sigma Aldrich or Fisher Scientific and were used without any further purification unless otherwise stated. The ZSM-5 zeolite sample (CBV 28014) with a silicon-to-aluminum ratio (SAR) of 140 was provided by Zeolyst International. The ammonium form of as received zeolite was calcined at 823 K for 6 h to obtain H-ZSM-5 under airflow.

Catalyst synthesis. Copper modified H-ZSM-5 zeolite catalyst was synthesized using modified ammonia evaporation method.[35,33] In a typical synthesis, 0.76 g copper nitrate was dissolved in 4 mL of water per g of H-ZSM-5 and the pH of the solution was maintained at 9.1 by adding an ammonia solution. Then, the final volume was made to 8 mL by adding deionized water. After that, 1 g of H-ZSM-5 zeolite was added to the solution and magnetically stirred at room temperature for 4 h. Finally, the mixture solution was kept at 353 K for 2 h in a closed vial with constant stirring before separating the solids with a centrifuge. After the centrifuging step, the liquid was decanted, and the remaining solids were washed with deionized water repeatedly until the pH of the solution reached 7. After drying in an oven overnight at 353 K, the catalyst was calcined at 823 K for 4 h under air flow (100 cm^3/min).

Catalyst characterizations. X-ray powder diffraction (XRD) measurements were performed on a PANalytical X-ray diffractometer using Cu Kα radiation source (λ=*0.15418 nm*). Brunauer-Emmett-Teller (BET) surface areas and pore volumes were determined from nitrogen

adsorption isotherms at 77 K using Autosorb-1 from Quantachrome Instruments. The copper loading was determined by inductively coupled plasma atomic emission spectroscopy (ICP-AES) at Galbraith Laboratories Inc. Thermogravimetric analysis (TGA) was completed using a TGA Q5000 (TA instrument, USA). The samples were heated to 573 K under helium and held for 30 h before ramping up to 1073 K at 5 K/min under air. The weight loss percentage during the heating under air was used to quantify the amount of coke deposited in the samples.[36] The morphology and elemental distribution of the fresh and the used catalysts were analyzed by a scanning transmission electron microscopy (STEM), FEI F200X Talos operating at 200 kV, equipped with an extreme field emission gun (X-FEG) electron source, high-angle annular dark-field (HAADF) detector and Super-X energy-dispersive X-ray spectroscopy (EDS) system with 4 silicon-drift detectors (SDD) (Bruker XFlash 120 mm^2) with a solid angle of 0.9 Steradian for chemical analysis. To avoid and/or decrease any potential electron beam damage during imaging and spectroscopy analysis, the current of the electron beam was controlled and was set to 250 pA. Part of the microscopy analysis was also performed on a JEOL 2200FS STEM/TEM instrument operating at 200 kV, equipped with a CEOS GmbH (Heidelberg, Ger) corrector on the illuminating lenses and EDS system (30mm^2 XFlash®5030 T Bruker). The imaging was performed in MAG 9C mode to achieve a low probe current of a nominal 14 pA. To optimize the count rate for X-ray HyperMaps acquisition, the beam conditions were switched to AMAG 5C imaging mode, yielding a beam with a nominal current of 140 pA. The specimen for STEM analysis were prepared by both microtomes (Leica EM UC7) and drop cast methods.

Catalyst performance testing. Conversion of 2,3-BDO was carried out in a tubular quartz reactor (1/2" O.D.) with a fix-bed configuration under ambient pressure. The reactor was vertically aligned in a temperature-controlled tubular furnace and a K-type thermocouple (Omega

Engineering) was placed in the middle of the reactor to measure the bed temperature. Typically, ~200 mg of catalyst was loaded after pelletizing and grounding into particle sizes of 125 to 250 μm. The catalyst was preheated to 573 K under hydrogen (10 cm^3/min) and argon (50 cm^3/min) flow and held for 90 min to reduce the copper oxides to metallic copper. After that, the temperature was lowered to reaction temperature (523 K). The 2,3-BDO was fed into the reactor using a syringe pump (KD Scientific) along with hydrogen. The products were analyzed with an on-line gas chromatograph equipped with a flame ionization detector (FID).

The 2,3-BDO conversion and product selectivity are calculated as follows:

$$\text{X}\ (\%) = \left[1 - \frac{n_{un}}{n_t}\right] \times 100\% \quad (1)$$

$$S_i\ (\%) = \left[\frac{n_i}{\sum_i n_i}\right] \times 100\% \quad (2)$$

Where X (%) is the 2,3-BDO conversion, n_{un} (mol) is the moles of carbon in unreacted 2,3-BDO, n_t (mol) is the moles of carbon in total 2,3-BDO feed, S_i (%) is the selectivity of product i, n_i (mol) is the moles of carbon in product i, $\sum_i n_i$ (mol) is the moles of carbon in all the products.

The oligomerization experiments were done in a high-pressure batch reactor (Parr Instrument). Propylene (Airgas, 10% in nitrogen), isobutene (Airgas, 99%), 1-butene (99.5%), trans-2-butene (>99%), cis-2-butene (>99%), 2-pentene (Sigma Aldrich, mixture of cis and trans, 99%) and 2-hexene (Sigma Aldrich, mixture of cis and trans, 85%) were used as the sources for $C_3^=$, $C_4^=$, $C_5^=$, and $C_6^=$, respectively. The olefin compositions used for the oligomerization reaction were based on normalizing the selectivity of each olefin over the total C_3-$C_6^=$ selectivity which was derived from the 2,3-BDO reaction and details are covered in the 'Oligomerization of C_3-$C_6^=$ to Jet-Range Hydrocarbons' section. In a typical reaction, the required amounts of olefin mixture

were introduced into the batch reactor with 10 g dried Amberlyst-36 (Sigma Aldrich) and heated to 423 K and hold for a different amount of time. When Amberlyst-15 (Sigma Aldrich) was used, the reaction temperature was 393 K. The products were analyzed with a gas chromatograph (Agilent 7820A) equipped with an FID detector. Product identification was done by injecting samples into the gas chromatograph (Agilent 6850) with a mass spectrometer (Agilent 5975C). C_7-C_{40} hydrocarbon standards (Sigma Aldrich) were also used to help with product determination.

Results and discussions

2,3-BDO conversion to C_{3+} olefins

Fresh catalyst characterizations: The first step of the 2,3-BDO to SAJF conversion pathway involves the formation of short-chain C_{3+} olefins (up to C_7 olefins) using Cu modified H-ZSM-5 catalyst (SAR=140, 13.3 wt.% Cu) which has been demonstrated by Zheng et al.[33,34] This catalyst is synthesized by a modified ammonia evaporation method and characterized to understand the zeolite structure and the copper distributions. Figure S1 shows the XRD patterns of the catalysts before and after Cu loading on H-ZSM-5 support. The deposition of copper over ZSM-5 support does not show any significant XRD pattern change indicating that the introduction of copper does not affect the structure of the parent H-ZSM-5 (Figure S1). Small decreases in BET surface areas (381 m^2/g for Cu/ZSM-5 and 408 m^2/g for H-ZSM-5) and micropore pore volumes (0.09 cm^3/g *vs.* 0.12 cm^3/g) after Cu loading (Table S1, Figure S2) are indicating that Cu might block some of the micropores. To get a better understanding of the Cu dispersion over ZSM-5 support, we also performed electron microscopy studies using STEM analysis. The low magnification HAADF-STEM images of Cu/ZSM-5 show micron-sized particles (Figure 1A). EDS mapping of these

particles shows that most of the copper tends to deposit on the outer layers as most of the nanoparticles range from 2 to 12 nm (Figure 1B and Figure S3).

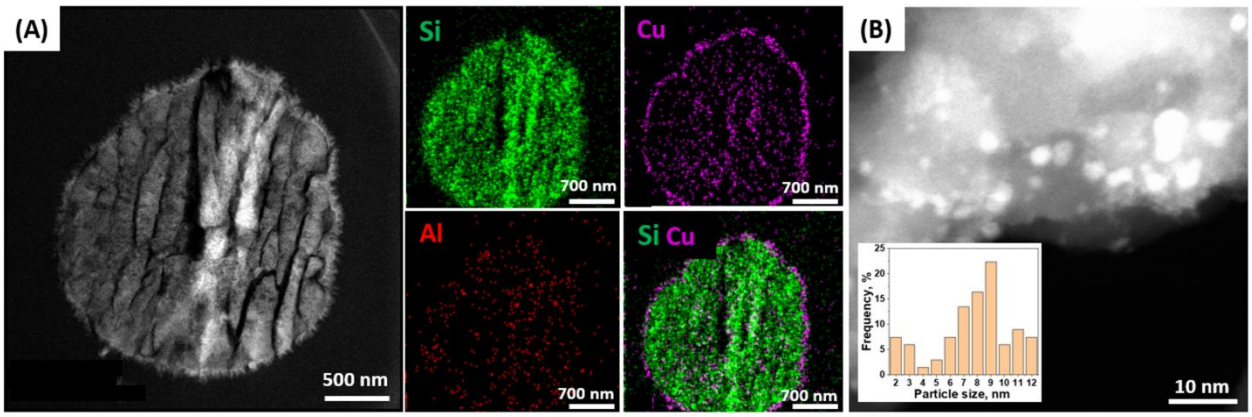

Figure 1. Electron microscopy characterization of Cu/ZSM-5. (A) Low magnification HAADF-STEM image of the catalyst particle cross-section with EDS HyperMaps showing distributions of Si, Al, and Cu; (B) Higher magnification HAADF-STEM image with the Cu particle size distributions on ZSM-5.

Product distributions: Figure 2 summarizes 2,3-BDO conversion and the product selectivity during ~40 h time on stream (TOS) over Cu/ZSM-5 catalyst at 523 K and 1.0 h^{-1} 2,3-BDO weight hourly space velocity (WHSV). Although butenes are obtained as the major products, significant amounts of other olefins ($C_3^=$, $C_5^=$, $C_6^=$, and $C_7^=$) are also observed with minor MEK at this reaction condition. The generally accepted reaction pathway for 2,3-BDO to butenes (and other olefins) is shown in Scheme S1.[24,37] MEK and 2-methyl propanal (MPA) are the initial dehydration products from 2,3-BDO.[37,38] Another possible product from 2,3-BDO dehydration is butadiene, which is formed by losing two water molecules during dehydration reactions.[15,23,26] The Brønsted acid sites present on the zeolite support are responsible for these dehydration reactions.[22,37,39] The fact that

we do not observe MPA and butadiene suggest the dehydration reaction over these Brønsted acid sites primarily favors MEK formation.[40] The Cu sites play a crucial role in the hydrogenation of the carbonyl group to convert MEK to 2-butanol,[33,41,42] which is further dehydrated to form butenes.[43] As shown in Scheme S1, butenes can go through various oligomerization reactions and cracking reactions to obtain $C_3^=$, $C_5^=$, $C_6^=$, and higher olefins (e.g., $C_7^=$) over the Brønsted acid sites.[44]

The 2,3-BDO conversion is kept above 97% with the total C_{3+} olefin selectivity maintained between 94% and 98% during ~40 h's reaction as shown in Figure 2A, which is much higher than other report[33,34] presumably due to higher hydrogen partial pressure (112 kPa) used in our study. Butenes selectivity increases with TOS and reaches more than 50% at 41 h while the selectivity for the sum of the $C_3^=$ and C_5-$C_7^=$ (downstream products from butene oligomerization and cracking) keep decreasing to 42% (Figure 2A). These results indicate the available Brønsted acid sites keep decreasing, most likely due to coke formation (discussed later), which slows down the butene oligomerization reaction. If we look into the distributions of butene isomers (Figure 2B), we can clearly see that the selectivities of cis-2-butene and trans-2-butenes increase with TOS (similar trend as the overall butene selectivity), while the selectivities of isobutene and 1-butene remain relatively constant, indicating the remaining Brønsted acid sites can still effectively catalyze the oligomerization of isobutene and 1-butene since these two butenes are much more reactive than 2-butenes during oligomerization.[45] Besides olefins, MEK selectivities remain almost constant (~2%) during ~40 hours' reaction (Figure 2A), which suggests the hydrogenation activity of Cu sites might not be affected significantly or the hydrogenation rate is still much higher than the rate-limiting step even if it decreases.

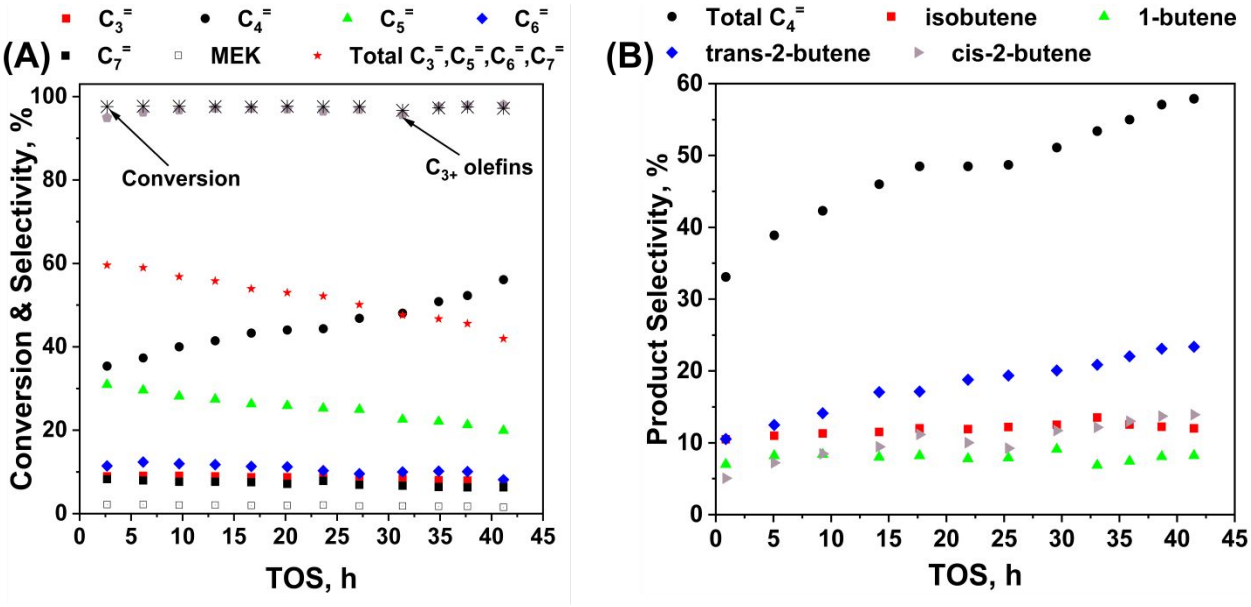

Figure 2. (A) 2,3-BDO conversion and product selectivities, (B) butene isomers selectivities over Cu/ZSM-5 catalyst for ~40 h TOS. Reaction conditions: pure 2,3-BDO, 523 K, 115 kPa, WHSV=1.0 h^{-1}, 2,3-BDO liquid flow rate is 0.2 mL/h, and hydrogen flow rate is 30 cm^3/min (hydrogen partial pressure is 112 kPa).

Effect of reaction conditions: Figure 3 shows the influence of H_2 partial pressure and reaction temperature on 2,3-BDO conversion and product selectivity. As shown in Figure 3A, lower H_2 partial pressure (37 kPa, balanced with Ar) favors the formation of $C_4^=$ and MEK while other olefins ($C_3^=$, $C_5^=$, $C_6^=$, and $C_7^=$) selectivities increase with increasing hydrogen partial pressure. The decrease of hydrogen partial pressure lowers the MEK hydrogenation activity as observed by the higher MEK selectivity at 37 kPa H_2 partial pressure. Conversion of 2,3-BDO under higher hydrogen partial pressure is the key to achieve high selectivity of C_{3+} olefins as demonstrated in this study as compared with other investigation[33,34].

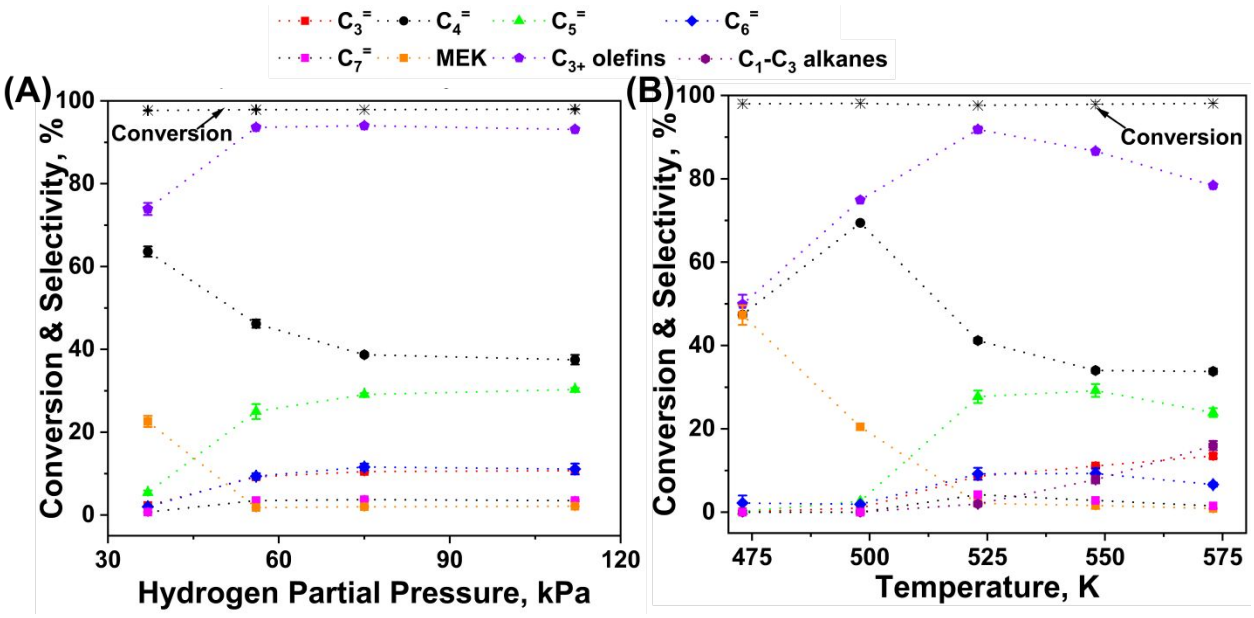

Figure 3. 2,3-BDO conversion and product selectivity as a function of (A) hydrogen partial pressure at 523 K, 115 kPa, WHSV=1.0 h^{-1}, 2,3-BDO liquid flow rate is 0.2 mL/h, and hydrogen flow rate is changed to vary the hydrogen partial pressure with total gas flow rate maintained at 30 cm^3/min (balanced by Ar). (B) Conversion and selectivity versus reaction temperature at 115 kPa, WHSV=1.0 h^{-1}, 2,3-BDO liquid flow rate is 0.2 mL/h, and hydrogen flow rate is 30 cm^3/min.

Besides hydrogen partial pressure, the impact of reaction temperature on the product selectivity is also studied. As shown in Figure 3B, the maximum C_{3+} olefins selectivity is observed at 523 K while lowering the temperature favors MEK formation due to reduced hydrogenation activity, with maximum MEK selectivity achieved as 47%. As the temperature increases from 473 to 548 K, the selectivities of other olefins ($C_3^=$, $C_5^=$, $C_6^=$, and $C_7^=$) increase. We also found that higher temperatures (548 K and 573 K) lead to the formation of C_1-C_3 light alkanes which might be due to cracking reactions, consistent with the findings of Zheng *et al*.[34] Based on these studies, we have shown that MEK could be optimized by varying the reaction conditions. Thus this process

offers flexibility to produce hydrocarbon fuels as well as valuable coproducts (MEK, an industrial solvent) by simply tuning the reaction conditions.

Effects of water and organic impurities: The separation and recovery of 2,3-BDO from the fermentation broth is challenging due to the presence of a large amount of water along with inorganic salts and organic side products/impurities.[30,46–49] In particular, the conventional distillation separation of 2,3-BDO from water is energy-intensive[30] because of the high boiling point of 2,3-BDO (450 K). An upgrading technology that can directly take aqueous 2,3-BDO as the feed will provide cost savings for the separation and purification processes. Hence, we performed the upgrading of aqueous 2,3-BDO to understand the impact of water on product selectivities and catalyst stability.

Figure 4 shows the product distributions in the presence of 40 wt.% water and the comparison with the run using pure 2,3-BDO. In both cases (with or without water), 2,3-BDO conversions are above 97% (Figure S4) and the selectivities for all the olefins show similar change trend between these runs, which suggests that water has a very minimal effect on product distributions for 2,3-BDO upgrading over Cu/ZSM-5 catalyst at this reaction condition for ~40 h TOS.

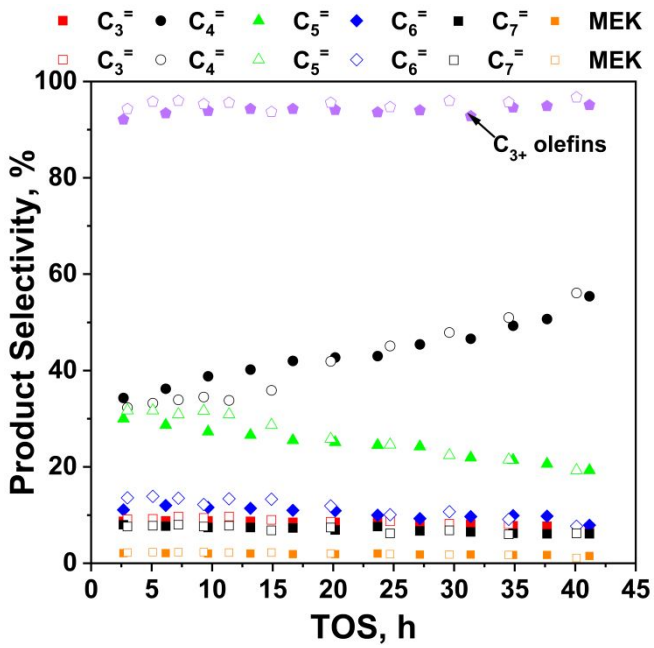

Figure 4. Product selectivities for reactions with pure 2,3-BDO feed (closed symbols) and 2,3-BDO with 40 wt.% water in the liquid feed (open symbols). Reaction conditions: 523 K, 115 kPa, 2,3-BDO WHSV=1.0 h^{-1}. For pure 2,3-BDO run, the liquid flow rate is 0.2 mL/h and H_2 gas flow rate is 30 cm^3/min. For the run with 40 wt.% water, the liquid flow rate is 0.33 mL/h and the H_2 gas flow rate is 27.1 cm^3/min.

Besides water, we also studied the effect of organic impurities on 2,3-BDO upgrading. Acetoin or acetic acid is added into the 2,3-BDO liquid feed as they are reported to be the major organic byproducts in the fermentation broth.[46] The conversion of 2,3-BDO is not affected by the introduction of organic impurities as shown in Figure S5A and S5B. In the case of co-feeding acetoin (10 wt.% acetoin/90 wt.% 2,3-BDO), the selectivities of total C_{3+} olefins, most of the individual olefins and MEK (Figure 5A) are all similar to the reaction with pure 2,3-BDO feed, indicating the presence of acetoin does not significantly affect the catalyst stability. To further

investigate this, we also fed aqueous acetoin alone (0.5 g acetoin/mL water) over Cu/ZSM-5 and found that the product distributions (Figure S6) are very similar to that observed in the pure 2,3-BDO run. It's very likely that acetoin is first hydrogenated to 2,3-BDO and then follows the same reaction pathway to form the olefin products as shown in Scheme S1. This is very important and useful for improving the carbon efficiency and the fuel yield by converting this type of organic byproduct to utilize more carbons from the fermentation broth.

We further investigated the impact of co-feeding 10 wt.% acetic acid on the product distributions during ~40 h TOS (Figure 5B and Figure S7). Although the 2,3-BDO conversion remains similarly as the run with pure 2,3-BDO (Figure S5B), the total C_{3+} olefin selectivity decreases drastically from 95% to 73% and MEK selectivity is boosted from 2% to 21% at early TOS (2.6 h) when co-feeding acetic acid (Figure 5B), revealing that the presence of acetic acid inhibits MEK hydrogenation. The $C_4^=$ selectivity is also significantly higher than that from pure 2,3-BDO run (66% vs 35% at 2.6 h) and becomes dominant among total C_{3+} olefins (Figure 5B). This is suggesting that acetic acid might also slow down the butene oligomerization due to direct interaction between acetic acid and the Brønsted acid sites (discussed further in the next section). Since the presence of acetic acid lowers the formation of C_{3+} olefins, removal of organic acid from the 2,3-BDO fermentation broth should be put into consideration when dealing with real biomass-derived 2,3-BDO.

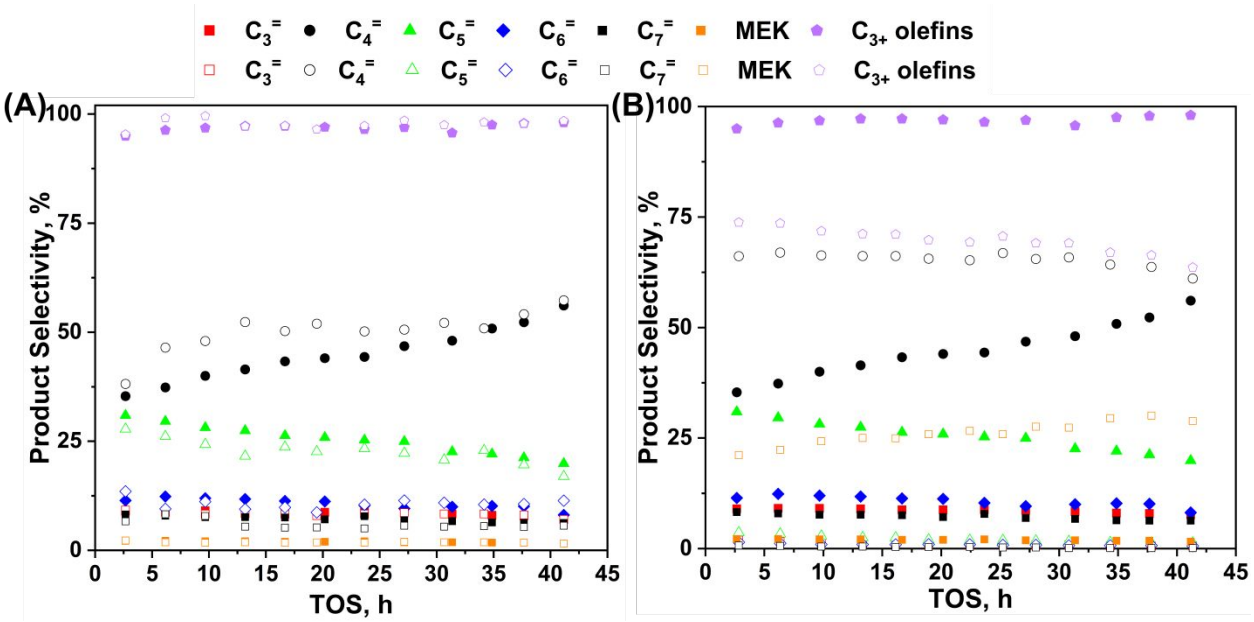

Figure 5. Product selectivities for 2,3-BDO conversion in the presence of organic impurities (open symbols) over Cu/ZSM-5 catalyst in comparison with pure 2,3-BDO run (closed symbols). (A) Co-feeding 10 wt.% acetoin, and (B) co-feeding 10 wt.% acetic acid. Reaction conditions: 523 K, 115 kPa, WHSV=1.0 h^{-1}, total liquid flow rate is 0.22 mL/h, and hydrogen flow rate is 30 cm^3/min.

Characterizations of the spent catalysts: The spent samples from the above runs were characterized to understand the changes in the zeolite structure and the Cu nanoparticles, along with the coke formation, which is used to correlate with the catalyst performance at different operating conditions. Zeolite structure is maintained after various durability studies under different conditions based on the XRD analysis of the spent samples (Figure S8). The new peak at ~37° (related to Cu_2O) shows up on the spent samples after running with co-feeding 40 wt.% water and co-feeding 10 wt.% acetic acid, indicating Cu sintering happens during these reactions. We performed HAADF-STEM analysis to further understand the changes of Cu nanoparticles during 2,3-BDO conversion. It was confirmed that the particle size increased on the samples running with 40 wt.% water and 10 wt.% acetic acid when compared with both spent sample running with pure

2,3-BDO and the fresh sample (Figure S9, Figure S3 and Figure 1), consistent with the XRD analysis. The fact that we did not observe a significant increase of MEK selectivity during the durability run with co-feeding 40 wt.% water (Figure 4), suggests the available Cu sites during the reactions are still sufficient to catalyze the hydrogenation of MEK despite Cu sintering. Of course, a long-term durability study (e.g., >1000 h) might be needed to further monitor the Cu site changes for future commercialization applications when dealing with the aqueous 2,3-BDO stream.

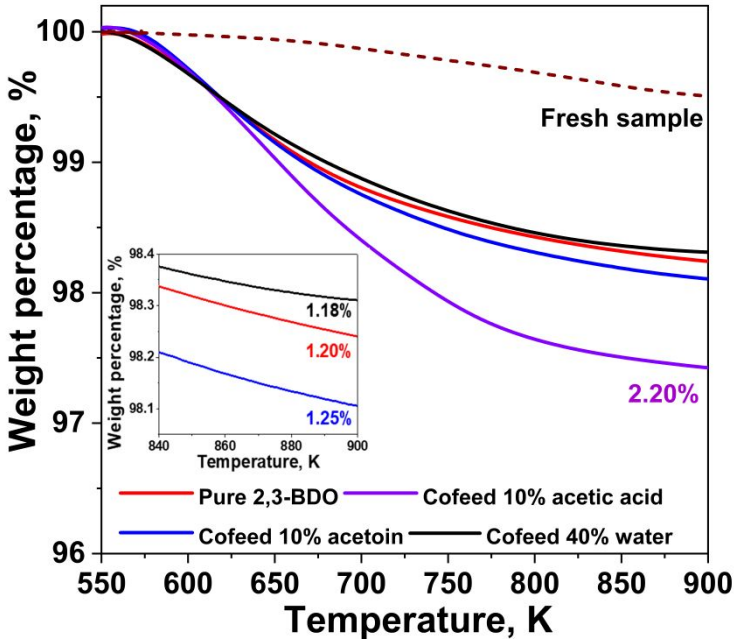

Figure 6. TGA analysis of the fresh Cu/ZSM-5 and spent Cu/ZSM-5 samples after ~40 h's reactions 1) with pure 2,3-BDO, 2) co-feeding 10 wt.% acetic acid, 3) co-feeding 10 wt.% acetoin, and 4) co-feeding 40 wt.% water.

The observation of increasing butene selectivity for the pure 2,3-BDO run (Figure 2) is likely due to coke formation as confirmed by the TGA analysis (1.2 wt.% coke formation after ~40 h run, Figure 6). The amounts of coke deposited for runs with pure 2,3-BDO, 10 wt.%

acetoin/90 wt.% 2,3-BDO and 40 wt.% water/60 wt.% 2,3-BDO are very similar (Figure 6), which is consistent with the observed similar butene selectivity changes among these runs. When comparing with pure 2,3-BDO run, butene selectivity increases significantly (Figure 5B) and the selectivity of non-butene C_{3+} olefins (sum of $C_3^=$, $C_5^=$, $C_6^=$, and $C_7^=$) decrease to 7.6% (Figure S10) at early TOS (2.6 h) in the presence of acetic acid. This indicates butene oligomerization activity is dramatically reduced when co-feeding acetic acid, which might be because the reaction of acetic acid with the Brønsted acid sites reduced the available acid sites for oligomerization reaction.[50] Gumidyala *et al.*[51] has reported acetic acid can form relatively stable acetyl species to replace some of the Brønsted acid sites over H-ZSM-5, which requires a higher temperature to recover, so that butene oligomerization is drastically inhibited. We have also observed that acetic acid is converted to ethyl acetate, ethylene, and ethane when co-feeding 10 wt.% acetic acid with 2,3-BDO (Figure S7). Similarly, ethyl acetate, ethylene, ethane, acetaldehyde, and acetone are produced when reacting pure acetic acid over Cu/ZSM-5 catalyst (Figure S11), where ethyl acetate is the major product for both cases. It has been reported that the production of ethyl acetate from acetic acid proceeds via the formation of surface acetyl species to replace the Brønsted acid sites,[50] supporting the hypothesis that the presence of acetic acid reduces the number of sites that are available for butene oligomerization. The sum of non-butene C_{3+} olefin ($C_3^=$, $C_5^=$, $C_6^=$, and $C_7^=$) selectivity decreases from 7.6% (2.6 h) to 2.5% (41 h) (67% decrease) (Figure S10) primarily due to the coke formation and we also found that the presence of 10 wt.% acetic acid accelerates the coke formation (Figure 6) compared with pure 2,3-BDO run. TGA analysis of the spent sample from reaction with pure acetic acid (same vapor phase concentration as pure 2,3-BDO run) also shows that acetic acid results in more coke formation than 2,3-BDO (Figure S12). This is consistent with

the finding of Vispute *et al*[52] that the hydrogen-deficient acetic acid tends to produce more coke than hydrogen-rich 2,3-BDO over H-ZSM-5 catalyst.

Overall, Cu/ZSM-5 catalyst can selectively make C_{3+} olefins (up to 98% selectivity) from 2,3-BDO with >97% conversion at 523 K, which is critical for producing a high yield of hydrocarbon fuels. Minimal impact from co-feeding water and acetoin offers the opportunity to apply this catalyst to the conversion of bio-derived 2,3-BDO. Of course, proper separation is needed to remove some inhibitors (e.g., acetic acid) when dealing with real biomass-derived 2,3-BDO. In order to further understand the type of fuels that could be made from these olefins, we moved on to study the oligomerization reaction (showed in the next section).

Oligomerization of C_3-$C_6^=$ to jet-range hydrocarbons

The second step of the 2,3-BDO to SAJF pathway involves the oligomerization of the short-chain olefins (C_3-$C_6^=$, the major olefins from 2,3-BDO conversion) to jet-range hydrocarbons (C_8-C_{16}). We demonstrated the oligomerization over Amberlyst-36 and Amberlyst-15 by using the mixed C_3-$C_6^=$ (similar composition as the C_3-$C_6^=$ distributions at 20 h TOS in Figure 2, also shown in Table S2). Table 1 and Table S3 show the hydrocarbon distributions from different oligomerization runs over Amberlyst-36 and Amberlyst-15. It is clear that the dominant fraction from all the oligomerization runs is in the jet range (C_8-C_{16}) with significant amounts of gasoline-range hydrocarbons (C_5-C_7) and minor C_{17}-C_{21} and C_{22+} hydrocarbons (Table S3). For jet-range hydrocarbons, C_8-C_{12} is dominating (Figure 7) for all the runs at different reaction conditions, which is consistent with other butene oligomerization reactions reported in the literature.[8,53–55] The carbon number distribution could be shifted to more C_{12+} by recycling C_7 and C_8 olefins[41] or

working with different oligomerization catalysts.[8,55,56] The major type of hydrocarbons is iso-olefins/isoparaffins with some amount of n-olefins/n-paraffins (Table 1), which can be readily hydrogenated to isoparaffins and n-paraffins respectively during the hydrogenation step. Small amounts of cyclic hydrocarbons and aromatics (Table S3) are also observed and typical hydrocarbon examples detected by GCMS are shown in Figure S13. The composition of petroleum-based jet fuel varies significantly depending on the crude oil used in the refining process,[57] but typically contains 60% of isoparaffins and n-paraffins,[58] 20% cyclic hydrocarbons with <25% aromatics, where the ratio among different non-aromatic hydrocarbons also varies dramatically. The fact that the oligomerization product rich in iso-olefins/isoparaffins and n-olefins/n-paraffins suggests the jet-range hydrocarbons derived from 2,3-BDO may be blended into petroleum jet at a high level.[58] Of course, detailed fuel property analysis will be needed in the future to determine the exact amount of blending. Different oligomerization catalysts and operation conditions could be employed to vary the type of hydrocarbons to meet the fuel properties if needed.[59]

Table 1. Product selectivities of hydrocarbons obtained from different oligomerization runs.

Run	Composition and reaction time	(C_5-C_7) wt.%	(C_8-C_{16}) wt.%	Iso-olefins/ isoparaffins wt.%	N-olefins/ n-paraffins wt.%
Olig 1[a]	C_3-$C_6^=$ mixture, 3 h	20.8 ± 0.3	70.0 ± 3.1	78.7 ± 1.0	10.3 ± 1.5
Olig 2[a]	C_3-$C_6^=$ mixture, 6 h	21.9 ± 0.4	70.6 ± 3.2	80.2 ± 1.0	11.0 ± 1.8
Olig 3[a]	C_3-$C_6^=$ mixture, 11 h	24.9 ± 0.4	64.5 ± 2.9	80.3 ± 1.0	5.5 ± 0.9
Olig 4[a]	$C_4^=$ only, 6 h	19.0 ± 0.3	65.2 ± 2.9	81.1 ± 1.0	6.9 ± 1.1
Olig 5[b]	C_3-$C_6^=$ mixture, 6 h	25.5 ± 0.4	67.3 ± 3.1	83.5 ± 1.0	7.7 ± 1.2

Conversions of the olefins are all >99%. The mass balance is 94-98% for all the runs. [a]Olig.1 to Olig. 4 were performed over Amberlyst-36 catalyst at 423 K and 42 bar at 281 K. [b]Olig. 5 was carried out over Amberlyst-15 catalyst at 393 K and 42 bar at 281 K.

When increasing the reaction time from 3 to 11 h (Olig 1 & 3), the selectivity of C_8-C_{16} hydrocarbons decreases to 64.5% at 11 h while the total C_5-C_7 increases from 20.8% to 24.9% (Table 1). Decrease of C_8-C_{16} hydrocarbons is observed when the olefins feed is changed from mixed C_3-C_6 olefins to butenes alone, however, the selectivity of iso-olefins/isoparaffins and n-olefins/n-paraffins does not change significantly (Olig 2 vs 4). When we change the catalyst from Amberlyst-36 to Amberlyst-15 under their maximum operating temperatures (Olig 2 vs 5), a slight increase of C_5-C_7 takes place along with shifting the type of hydrocarbons to more iso-olefins/isoparaffins.

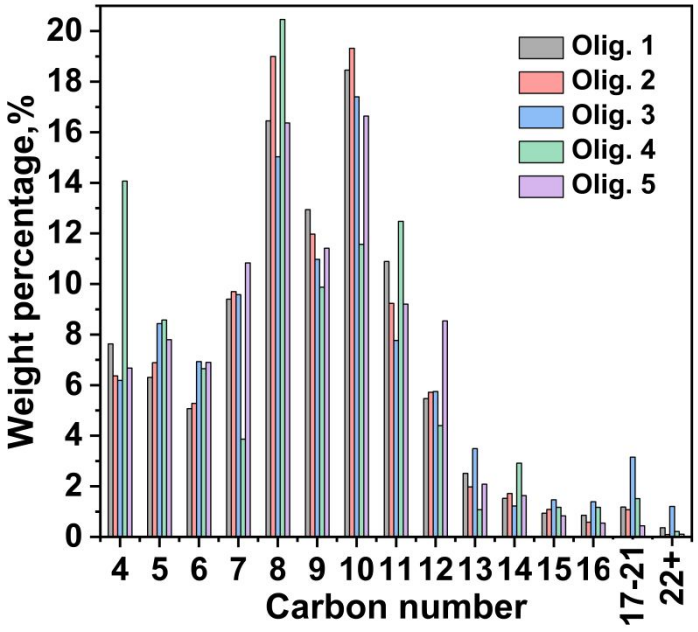

Figure 7. Carbon number distributions from different oligomerization runs.

Discussion of the integrated process

Carbon efficiency and product yield for each step of the integrated pathway of biomass to liquid hydrocarbon fuels via 2,3-BDO are summarized in Figure 8 and Table 2. Biomass (corn stover as an example) is first fractionated to cellulose/hemicellulose and lignin after pretreatment, followed by enzymatic hydrolysis and fermentation to produce 2,3-BDO from sugars (not the focus of this study).[16] Then 2,3-BDO is converted to $C_{3+}^{=}$ over Cu/ZSM-5 catalyst with carbon efficiency and product mass yield of 95% and 59%, respectively (41 h TOS, Figure 2). Oligomerization is carried out to upgrade these mixed olefins to C_{5+} hydrocarbons using Amberlyst-36 catalyst, where carbon efficiencies for the C_{5+} hydrocarbons and the C_8-C_{16} jet-range hydrocarbons are 94% and 71%, respectively. Hydrogenation of the olefins is a well-demonstrated process (not investigated in this work) with the assumption of 99% carbon efficiency.[16] For the whole process, the carbon efficiency and the fuel yield (from dry biomass) of C_{5+} hydrocarbons are 25-28% and 12-15% (0.12-0.15 g/g dry biomass, or 39.4-49.3 gallon fuel/dry ton biomass), respectively, while the jet-range hydrocarbon yield is 29.6-36.1 gallon fuel/dry ton biomass. The theoretical maximum carbon efficiency of C_{5+} hydrocarbons from corn stover is 34% if we assume 51% sugar recovery from corn stover, 67% 2,3-BDO from fermentation and 100% efficiency for all the catalytic conversion steps. Our reported carbon efficiency of C_{5+} hydrocarbons is 74-82% of the theoretical maximum efficiency. If sugar (e.g., glucose) is directly used as the feedstock, the overall carbon yield to liquid hydrocarbons is as high as 55-56%.

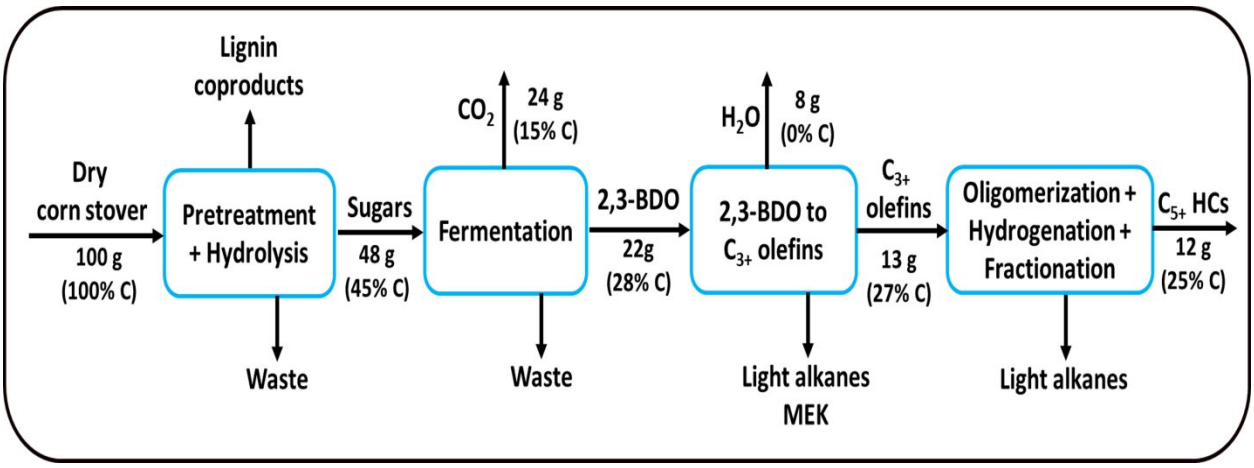

Figure 8. Process scheme for biomass conversion to liquid hydrocarbon fuels and lignin coproduct (e.g., adipic acid). The numbers used for biomass to sugars, fermentation and hydrotreating steps are estimated from the National Renewable Energy Laboratory (NREL) 2018 Biochemical Design Case report.[16] C_{3+} olefins yield during '2,3-BDO to C_{3+} olefins' step is the data at 41 h TOS shown in Figure 2. Oligomerization product yields are based on the results from Olig 2 run in this work. Process loss is not considered for the calculations.

Table 2. Carbon efficiency and product mass yield for each step of 2,3-BDO to jet fuel pathway.

Step	Carbon Efficiency (mol C in product/mol C in feed)	Mass yield (g product/g dry feed)
Biomass to sugars [a]	0.45 [b] -0.51 [c]	0.48 [b]-0.54 [c]
Sugars to 2,3-BDO via fermentation[16]	0.62 [b] -0.64 [c]	0.45 [b]-0.48 [c]
2,3-BDO to C_{3+} olefins [d]	0.95	0.59
Oligomerization to C_{5+} [e]	0.94	0.94
Oligomerization to C_8-C_{16} [e]	0.71	0.71
Hydrogenation[41]	0.99 [b]	1.04 [b]

Overall (to C_{5+} hydrocarbons) [f]	0.25-0.28 (0.55-0.56) [g]	0.12-0.15 (0.26-0.27) [g]
Overall (to C_8-C_{16} hydrocarbons) [h]	0.19-0.22 (0.41-0.43) [g]	0.09-0.11 (0.19-0.20) [g]

[a] Corn stover is used as the feedstock. Biomass to sugars includes pretreatment and hydrolysis steps. [b] Estimated based on the NREL 2018 Biochemical Design Case report.[16] [c] Year 2030 target as shown in the NREL 2018 Biochemical Design Case report.[16] [d] Yield of C_{3+} olefins at 41 h TOS shown in Figure 2. [e] These calculations are based on the results from Olig 2 run in our work. [f] Calculated by multiplying the carbon efficiency or weight yield: (biomass to sugars) × (sugars to 2,3-BDO via fermentation) × (2,3-BDO to C_{3+} olefins) × (oligomerization to C_{5+}) × (hydrogenation). [g] The numbers inside the parentheses represent the efficiency and yield when using glucose as the feedstock. [h] Calculated by multiplying the carbon efficiency or weight yield: (biomass to sugars) × (sugars to 2,3-BDO via fermentation) × (2,3-BDO to C_{3+} olefins) × (oligomerization to C_8-C_{16}) × (hydrogenation).

Ethanol to jet fuel, another type of hybrid pathway when ethanol is derived from the fermentation process, has been widely studied and reported.[3,5,60] Table S4 and Table S5 report the carbon efficiency for ethanol to jet fuel via ethanol dehydration[61], ethylene dimerization over H-SSZ-13[62] and further oligomerizations to jet-range hydrocarbons. The yields of total liquid hydrocarbons and jet fuel are all lower than those for the 2,3-BDO pathway primarily due to lower C_{3+} olefins yield from ethylene conversion (per pass) (Table S5). Separation and recycling of ethylene from C_{3+} olefins are needed to further enhance the C_{3+} olefin yield, leading to an increase of both capital and operating expenses. Similar to the hybrid routes, the aqueous-phase routes primarily utilize the cellulose and hemicellulose fractions.[63] Here we compare with three reported aqueous-phase pathways: 1) biomass conversion to GVL, further converted to butenes, followed by butene oligomerization[8] and hydrogenation (Table S6); 2) biomass to GVL, followed by conversion to 5-nonanone and then form hydrocarbons via hydrogenation[64] (Table S7); 3) biomass to HMF/furfural, followed by aldol condensation and hydrotreating[11] (Table S8). All the reported carbon efficiency and fuel yield of total liquid hydrocarbons and jet-range hydrocarbons are similar to ethanol to jet pathway, but lower than 2,3-BDO pathway.

Thermochemical upgrading pathways, including catalytic fast pyrolysis + hydrotreating, pyrolysis + hydrodeoxygenation, and gasification + syngas to jet via olefin intermediates (Table S9), could utilize the whole biomass and they may offer a higher yield of liquid hydrocarbon fuels due to the utilization of lignin. Catalytic fast pyrolysis + hydrotreating and pyrolysis + hydrodeoxygenation are reported to show higher carbon efficiency for the total liquid hydrocarbons with certain optimum catalysts and processes conditions.[12,13] The liquid fuels from these pathways are dominant with gasoline and diesel fractions[12] while jet-range hydrocarbon yield is less than the other pathways. For both the hybrid routes and the aqueous-phase routes, lignin fraction is available either after the pretreatment step or after fermentation[65,66] as important feedstocks for many potential applications. Effective utilization of the fractionated lignin could increase the overall carbon efficiency of biomass conversion and produce high-value coproducts to reduce the fuel production cost.[67] Adipic acid (a high-value coproduct), for example, has been shown to be produced via metabolic engineering, separations, and catalysis.[68] Based on NREL's 2018 Biochemical Design Case report, the projected adipic acid production from lignin could reach a carbon efficiency of 15% (based on dry biomass), which will increase the total carbon efficiency of biomass to liquid fuels and coproduct to 40-43%,[16] exceeding most of the thermochemical routes. All of these comparisons, taken together, have suggested biomass conversion to liquid hydrocarbon fuels (including jet fuel) via 2,3-BDO is one of the promising pathways that could deliver high carbon conversion efficiency and offer the potential to generate valuable co-products (e.g., MEK and adipic acid), which could help to improve the overall process economics.

Conclusions

In summary, we have demonstrated a hybrid pathway of biomass conversion to liquid hydrocarbon fuels via a 2,3-BDO platform which offers a high carbon efficiency and opportunities to produce high-value co-products to improve the overall process economics. The first step involves the conversion of 2,3-BDO to C_{3+} olefins, where Cu/ZSM-5 can achieve 98% selectivity of C_{3+} olefins with ~97% 2,3-BDO conversion at 41 h TOS. The product distributions can be tuned to obtain coproducts like MEK by varying the reaction conditions, enhancing the process flexibility between making fuel products and other value-added coproducts. Catalyst stability is not affected by the presence of 40 wt.% water or 10 wt.% acetoin, however, co-feeding 10 wt.% of acetic acid in the 2,3-BDO feed decreases the selectivity of C_{3+} olefins and accelerates the coke formation. These studies provide important guidance for upgrading real biomass-derived 2,3-BDO and separation of 2,3-BDO from the fermentation broth. The C_3-$C_6^=$ olefins obtained from the BTO step is further oligomerized to form 94% of C_{5+} liquid hydrocarbon fuels with 71% jet-range hydrocarbons. The carbon efficiency for the integrated biomass to fuels via 2,3-BDO has been shown to be 25-28% when using corn stover as the feedstock, showing great advantages when compared with other routes of biomass to liquid hydrocarbon fuels.

Conflicts of Interest

The authors declare no competing financial interest.

Acknowledgments

This research is sponsored by the U.S. Department of Energy (DOE), Office of Energy Efficiency and Renewable Energy, BioEnergy Technologies Office, under contract DE-AC05-00OR22725 with UT-Battelle, LLC, and in collaboration with the Chemical Catalysis for Bioenergy (ChemCatBio) Consortium, a member of the Energy Materials Network. Microscopy research was supported by the Office of Nuclear Energy, Fuel Cycle R&D Program and the Nuclear Science User Facilities. The author would like to thank Min Zhang and Rick Elander at NREL for discussion on biomass pretreatment, hydrolysis, and fermentation, thank S. K. Reeves at ORNL for assistance with the experimental work and Mi Lu for comments on the manuscript. The views and opinions of the authors expressed herein do not necessarily state or reflect those of the United States Government or any agency thereof.

References

1 C. Gutiérrez-Antonio, F. I. Gómez-Castro, J. A. de Lira-Flores and S. Hernández, *Renew. Sust. Energ. Rev.*, 2017, **79**, 709–729.
2 N. R. Baral, O. Kavvada, D. Mendez-Perez, A. Mukhopadhyay, T. S. Lee, B. A. Simmons and C. D. Scown, *Energy Environ. Sci.*, 2019, **12**, 807–824.
3 W.-C. Wang, L. Tao, J. Markham, Y. Zhang, E. Tan, L. Batan, E. Warner and M. Biddy, *Review of Biojet Fuel Conversion Technologies*, United States, 2016.
4 G. W. Huber, S. Iborra and A. Corma, *Chem. Rev.*, 2006, **106**, 4044–4098.
5 W.-C. Wang and L. Tao, *Renew. Sust. Energ. Rev.*, 2016, **53**, 801–822.
6 K. Kumar, F. Parveen, T. Patra and S. Upadhyayula, *New J. Chem.*, 2018, **42**, 228–236.
7 C. Moreno-Marrodan and P. Barbaro, *Green Chem.*, 2014, **16**, 3434–3438.
8 J. Q. Bond, D. M. Alonso, D. Wang, R. M. West and J. A. Dumesic, *Science*, 2010, **327**, 1110–1114.
9 M. Moliner, Y. Román-Leshkov and M. E. Davis, *Proc. Natl. Acad. Sci. U. S. A.*, 2010, **107**, 6164–6168.
10 W. Aehle, Enzymes in Industry: Production and Applications, 3rd Edition.
11 R. M. West, Z. Y. Liu, M. Peter and J. A. Dumesic, *ChemSusChem*, 2008, **1**, 417–424.
12 M. B. Griffin, K. Iisa, H. Wang, A. Dutta, K. A. Orton, R. J. French, D. M. Santosa, N. Wilson, E. Christensen, C. Nash, K. M. Van Allsburg, F. G. Baddour, D. A. Ruddy, E. C. D. Tan, H. Cai, C. Mukarakate and J. A. Schaidle, *Energy Environ. Sci.*, 2018, **11**, 2904–2918.

13 D. C. Elliott, H. Wang, R. French, S. Deutch and K. Iisa, *Energy Fuels*, 2014, **28**, 5909–5917.
14 V. L. Dagle, C. Smith, M. Flake, K. O. Albrecht, M. J. Gray, K. K. Ramasamy and R. A. Dagle, *Green Chem.*, 2016, **18**, 1880–1891.
15 J. Han, L. Tao and M. Wang, *Biotechnol Biofuels*, 2017, **10**, 21.
16 R. E. Davis, N. J. Grundl, L. Tao, M. J. Biddy, E. C. Tan, G. T. Beckham, D. Humbird, D. N. Thompson and M. S. Roni, *Process Design and Economics for the Conversion of Lignocellulosic Biomass to Hydrocarbon Fuels and Coproducts: 2018 Biochemical Design Case Update; Biochemical Deconstruction and Conversion of Biomass to Fuels and Products via Integrated Biorefinery Pathways*, 2018.
17 L. Wu, T. Moteki, A. A. Gokhale, D. W. Flaherty and F. D. Toste, *Chem*, 2016, **1**, 32–58.
18 *Alternative Aviation Fuels: Overview of Challenges, Opportunities, and Next Steps, DOE/EE--1515, 1358063*, 2017.
19 A. M. Bialkowska, *World. J. Microbiol. Biotechnol.*, 2016, **32**, 200.
20 M. Köpke, C. Mihalcea, F. Liew, J. H. Tizard, M. S. Ali, J. J. Conolly, B. Al-Sinawi and S. D. Simpson, *Appl. Environ. Microbiol.*, 2011, **77**, 5467.
21 Á. Fernández-Naveira, H. N. Abubackar, M. C. Veiga and C. Kennes, *World. J. Microbiol. Biotechnol.*, 2017, **33**, 43.
22 X.-J. Ji, H. Huang and P.-K. Ouyang, *Biotechnol. Adv.*, 2011, **29**, 351–364.
23 S. Cho, T. Kim, H. M. Woo, Y. Kim, J. Lee and Y. Um, *Biotechnol Biofuels*, 2015, **8**, 146.
24 J. Zhao, D. Yu, W. Zhang, Y. Hu, T. Jiang, J. Fu and H. Huang, *RSC Adv.*, 2016, **6**, 16988–16995.
25 J. van Haveren, E. L. Scott and J. Sanders, *Biofuel Bioprod Biorefin*, 2008, **2**, 41–57.
26 X. Liu, V. Fabos, S. Taylor, D. W. Knight, K. Whiston and G. J. Hutchings, *Chem.--Eur. J.*, 2016, **22**, 12290–12294.
27 M. J. Biddy, C. Scarlata and C. Kinchin, *Chemicals from Biomass: A Market Assessment of Bioproducts with Near-Term Potential*, United States, 2016.
28 E. Celińska and W. Grajek, *Biotechnol. Adv.*, 2009, **27**, 715–725.
29 Butanediol (1,4 BDO & 2,3 BDO) 1,3 Butadiene and Methyl Ethyl Ketone (MEK) Market-Market Size and Forecast 2010-2018, https://www.transparencymarketresearch.com/butanediol-butadiene-and-mek-market.html.
30 G. R. Harvianto, J. Haider, J. Hong, N. Van Duc Long, J.-J. Shim, M. H. Cho, W. K. Kim and M. Lee, *Biotechnol Biofuels*, 2018, **11**, 18.
31 F. Jing, B. Katryniok, M. Araque, R. Wojcieszak, M. Capron, S. Paul, M. Daturi, J.-M. Clacens, F. De Campo, A. Liebens, F. Dumeignil and M. Pera-Titus, *Catal. Sci. Technol.*, 2016, **6**, 5830–5840.
32 D. Tsukamoto, S. Sakami, M. Ito, K. Yamada and T. Yonehara, *Chem. Lett.*, 2016, **45**, 831–833.
33 Q. Zheng, J. Grossardt, H. Almkhelfe, J. Xu, B. P. Grady, J. T. Douglas, P. B. Amama and K. L. Hohn, *J. Catal.*, 2017, **354**, 182–196.
34 Q. Zheng, M. D. Wales, M. G. Heidlage, M. Rezac, H. Wang, S. H. Bossmann and K. L. Hohn, *J. Catal.*, 2015, **330**, 222–237.
35 S. Shwan, M. Skoglundh, L. F. Lundegaard, R. R. Tiruvalam, T. V. W. Janssens, A. Carlsson and P. N. R. Vennestrøm, *ACS Catal.*, 2015, **5**, 16–19.
36 D. Rojo-Gama, M. Signorile, F. Bonino, S. Bordiga, U. Olsbye, K. P. Lillerud, P. Beato and S. Svelle, *J. Catal.*, 2017, **351**, 33–48.

37 W. Zhang, D. Yu, X. Ji and H. Huang, *Green Chem.*, 2012, **14**, 3441–3450.
38 A. V. Tran and R. P. Chambers, *Biotechnol. Bioeng.*, 1987, **29**, 343–351.
39 H. Duan, Y. Yamada and S. Sato, *Appl. Catal., A*, 2015, **491**, 163–169.
40 M. A. Nikitina, V. L. Sushkevich and I. I. Ivanova, *Pet. Chem.*, 2016, **56**, 230–236.
41 S. Zhang, H. Ma, Y. Sun, Y. Luo, X. Liu, M. Zhang, J. Gao and J. Xu, *Green Chem.*, 2019, **21**, 1702–1709.
42 N. Gorgas, B. Stöger, L. F. Veiros and K. Kirchner, *ACS Catal.*, 2016, **6**, 2664–2672.
43 D. Zhang, R. Al-Hajri, S. A. I. Barri and D. Chadwick, *Chem. Commun.*, 2010, **46**, 4088–4090.
44 C.-J. Chen, S. Rangarajan, I. M. Hill and A. Bhan, *ACS Catal.*, 2014, **4**, 2319–2327.
45 A. Ehrmaier, Y. Liu, S. Peitz, A. Jentys, Y.-H. C. Chin, M. Sanchez-Sanchez, R. Bermejo-Deval and J. Lercher, *ACS Catal.*, 2019, **9**, 315–324.
46 S. Jeon, D.-K. Kim, H. Song, H. J. Lee, S. Park, D. Seung and Y. K. Chang, *J. Biosci. Bioeng.*, 2014, **117**, 464–470.
47 Y. Li, J. Zhu, Y. Wu and J. Liu, *Korean J. Chem. Eng.*, 2013, **30**, 73–81.
48 Y. Li, Y. Wu, J. Zhu, J. Liu and Y. Shen, *Journal of Saudi Chemical Society*, 2016, **20**, S495–S502.
49 Y. Li, Y. Wu, J. Zhu and J. Liu, *Biotechnol. Bioprocess Eng.*, 2012, **17**, 337–345.
50 J. Bedard, H. Chiang and A. Bhan, *J. Catal.*, 2012, **290**, 210–219.
51 A. Gumidyala, T. Sooknoi and S. Crossley, *J. Catal.*, 2016, **340**, 76–84.
52 T. P. Vispute, H. Zhang, A. Sanna, R. Xiao and G. W. Huber, *Science*, 2010, **330**, 1222–1227.
53 J. Saavedra Lopez, R. A. Dagle, V. L. Dagle, C. Smith and K. O. Albrecht, *Catal. Sci. Technol.*, 2019, **9**, 1117–1131.
54 Z. Xu, J. P. Chada, D. Zhao, C. A. Carrero, Y. T. Kim, D. C. Rosenfeld, J. L. Rogers, S. J. Rozeveld, I. Hermans and G. W. Huber, *ACS Catal.*, 2016, **6**, 3815–3825.
55 D. Lee, H. Kim, Y.-K. Park and J.-K. Jeon, *Catalysts*, , DOI:10.3390/catal8100456.
56 W. Monama, E. Mohiuddin, B. Thangaraj, M. M. Mdleleni and D. Key, *Catal. Today*, 2020, **342**, 167–177.
57 S. Blakey, L. Rye and C. W. Wilson, *Proceedings of the Combustion Institute*, 2011, **33**, 2863–2885.
58 B. Khandelwal, S. Roy, C. Lord and S. Blakey, *Aerospace*, 2014, **1**, 52–66.
59 M. L. Sarazen, E. Doskocil and E. Iglesia, *ACS Catal.*, 2016, **6**, 7059–7070.
60 N. M. Eagan, M. D. Kumbhalkar, J. S. Buchanan, J. A. Dumesic and G. W. Huber, *Nat. Rev. Chem.*, 2019, **3**, 223–249.
61 D. Varisli, T. Dogu and G. Dogu, *Ind. Eng. Chem. Res.*, 2008, **47**, 4071–4076.
62 W. Dai, X. Sun, B. Tang, G. Wu, L. Li, N. Guan and M. Hunger, *J. Catal.*, 2014, **314**, 10–20.
63 J. C. Serrano-Ruiz and J. A. Dumesic, *Energy Environ. Sci.*, 2011, **4**, 83–99.
64 J. C. Serrano-Ruiz, D. Wang and J. A. Dumesic, *Green Chem.*, 2010, **12**, 574–577.
65 I. Norberg, Y. Nordström, R. Drougge, G. Gellerstedt and E. Sjöholm, *J. Appl. Polym. Sci.*, 2013, **128**, 3824–3830.
66 A. J. Ragauskas, G. T. Beckham, M. J. Biddy, R. Chandra, F. Chen, M. F. Davis, B. H. Davison, R. A. Dixon, P. Gilna, M. Keller, P. Langan, A. K. Naskar, J. N. Saddler, T. J. Tschaplinski, G. A. Tuskan and C. E. Wyman, *Science*, , DOI:10.1126/science.1246843.

67 R. Davis, L. Tao, E. C. D. Tan, M. J. Biddy, G. T. Beckham, C. Scarlata, J. Jacobson, K. Cafferty, J. Ross, J. Lukas, D. Knorr and P. Schoen, *Process Design and Economics for the Conversion of Lignocellulosic Biomass to Hydrocarbons: Dilute-Acid and Enzymatic Deconstruction of Biomass to Sugars and Biological Conversion of Sugars to Hydrocarbons*, United States, 2013.

68 D. R. Vardon, M. A. Franden, C. W. Johnson, E. M. Karp, M. T. Guarnieri, J. G. Linger, M. J. Salm, T. J. Strathmann and G. T. Beckham, *Energy Environ. Sci.*, 2015, **8**, 617–628.

TOC Entry:

A new hybrid pathway to biojet fuel via biomass-derived 2,3-butanediol has been demonstrated with high carbon recovery (74-82% of the theoretical maximum efficiency).